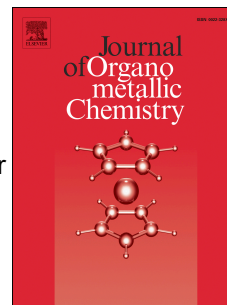


Accepted Manuscript

Ruthenium(0) complexes with triazolylidene spectator ligands: Oxidative activation for (de)hydrogenation catalysis

Cristiana Cesari, Rita Mazzoni, Helge Müller-Bunz, Martin Albrecht



PII: S0022-328X(15)00090-X

DOI: [10.1016/j.jorganchem.2015.02.022](https://doi.org/10.1016/j.jorganchem.2015.02.022)

Reference: JOM 18922

To appear in: *Journal of Organometallic Chemistry*

Received Date: 15 January 2015

Revised Date: 9 February 2015

Accepted Date: 13 February 2015

Please cite this article as: C. Cesari, R. Mazzoni, H. Müller-Bunz, M. Albrecht, Ruthenium(0) complexes with triazolylidene spectator ligands: Oxidative activation for (de)hydrogenation catalysis, *Journal of Organometallic Chemistry* (2015), doi: 10.1016/j.jorganchem.2015.02.022.

This is a PDF file of an unedited manuscript that has been accepted for publication. As a service to our customers we are providing this early version of the manuscript. The manuscript will undergo copyediting, typesetting, and review of the resulting proof before it is published in its final form. Please note that during the production process errors may be discovered which could affect the content, and all legal disclaimers that apply to the journal pertain.

Ruthenium(0) complexes with triazolylidene spectator ligands: oxidative activation for (de)hydrogenation catalysis

Cristiana Cesari,^{a,b} Rita Mazzoni,^b Helge Müller-Bunz,^a Martin Albrecht^{*,a}

a) School of Chemistry & Chemical Biology, University College Dublin, Belfield, Dublin 4, Ireland

b) Dipartimento di Chimica Industriale "Toso Montanari", viale Risorgimento 4, 40136 Bologna, Italy

Author contact: E-mail: martin.albrecht@ucd.ie; Fax: +353 17162501

In memoriam A. E. Shilov in recognition and admiration of his pioneering work on C–H bond activation.

Abstract

Transmetallation of silver triazolylidene intermediates with the ruthenium(0) precursor [Ru(Cp=O)(CO)₂]₂ afforded low-valent ruthenium(0) complexes containing a triazole-derived NHC ligand (Cp=O = 3,4-di(4-methoxyphenyl)-2,5-diphenyl-cyclopentadienone). Protonation of the carbonyl group of the Cp=O ligand significantly reduces the π character of the Ru–CO bond as deduced from ν_{CO} analysis. The new triazolylidene ruthenium(0) complexes were evaluated as catalyst precursors in transfer hydrogenation of 4-fluoro-acetophenone and in the acceptorless dehydrogenation of benzyl alcohol. Low activities were noted, though in both reactions, catalytic performance is markedly increased when cerium(IV) was added. Electrochemical analysis indicate that activation of the catalyst precursor proceeds via cerium-mediated oxidation of the ruthenium center, which facilitates dissociation of a CO ligand to enter the catalytic cycle. Such oxidative activation of catalyst precursors may be of more general scope.

Keywords

Ruthenium – N-heterocyclic carbenes – mesoionic triazolylidenes – oxidative activation – alcohol dehydrogenation – transfer hydrogenation

Introduction

N-Heterocyclic carbenes (NHCs) have become some of the most popular ligands in transition metal chemistry due to their efficiency as ancillary ligands to improve catalytic activity.¹ Their success is due to a combination of unique properties, such as their easily tunable electronic and steric properties that influence the metal center and which allow catalytic activity to be rationally optimized. The exploitation of such concepts is particularly appealing because the synthesis of NHC ligand precursors as well as NHC metal complexes is fairly simple and highly versatile.²

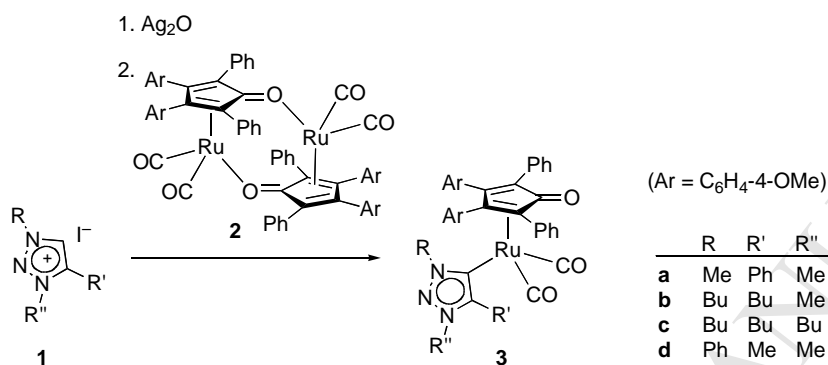
Accordingly, a variety of catalytic reactions have strongly benefited from introduction of NHC ligands, such as ruthenium-catalyzed olefin metathesis,³ palladium-catalyzed cross-coupling reactions,⁴ iridium-catalyzed reductions and oxidations,⁵ and gold-catalyzed activation of π -bonds, to name but a few.⁶ Apart from olefin metathesis, NHC ruthenium complexes have shown catalytic activity in various redox transformations,⁷ including: transfer hydrogenation,⁸ hydrogenation of olefins⁹ and esters,¹⁰ asymmetric hydrogenation,¹¹ amide synthesis from alcohols and nitriles,¹² dehydrogenation of esters and imines from alcohols,¹³ racemization of chiral alcohols,¹⁴ oxidation of alcohols¹⁵ and water oxidation.¹⁶ Most of the literature on NHC ruthenium chemistry features ruthenium(II) complexes, while low-valent NHC ruthenium(0) systems are restricted to a few examples based on either $[\text{Ru}_3(\text{CO})_{12}]$ or $[\text{Ru}(\text{CO})_2(\text{PPh}_3)_3]$ as precursors.¹⁷ Recently, a straightforward approach towards NHC ruthenium(0) complexes has been developed,¹⁸ which is based on a dimeric ruthenium(0) cyclopentadienone dicarbonyl dimer.¹⁹ Cleavage of the dimer in the presence of a free carbene or a silver carbene precursor provided access to a new class of ruthenium complexes.

Here we have expanded this synthetic methodology to 1,2,3-triazolylienes as strong donor NHC-type ligands.²⁰ Triazolylienes offer a vast synthetic flexibility due to their convenient accessibility through [2+3] dipolar cycloaddition of alkynes and azides.²¹ In addition, their enhanced donor properties as compared to more commonly utilized imidazolylienes may further destabilize the ruthenium(0) oxidation state and hence facilitate substrate activation by metal/ligand cooperation in analogy to the reduced portion of Shvo's catalyst.²² Thus, it will be of particular interest to evaluate the propensity of the new triazolyliene ruthenium(0) complexes to dehydrogenate substrates via formal H_2 transfer, as this process may lead to efficient catalysts for acceptorless oxidation (alcohol dehydrogenation) or transfer hydrogenation.

Results and Discussion

Synthesis of triazolylidene Ru complexes

The triazolium salts **1a-d**, readily accessible by “click” cycloaddition of the corresponding alkynes and azides and subsequent alkylation,²¹ were successfully transformed into the silver triazolylidene intermediates as reported previously.²³ Transmetalation with the low-valent ruthenium precursor afforded complexes **3a-d** in very high yields (Scheme 1). Complexes **3** constitute a class of ruthenium(0) complexes which contain exclusively carbon-donor ligands.



Scheme 1. Synthesis of cyclopentadienone triazolylidene ruthenium(0) complexes **3a-d**.

Formation of complexes **3a-d** was established by ¹H NMR, ¹³C{¹H} NMR, and IR spectroscopy as well as ESI-MS and for representative examples, by single crystal X-ray diffraction analysis. IR spectroscopy provided a particularly convenient methodology for monitoring the progress of the transmetalation reaction, as the Ru–CO vibrations of the precursor complex shifted distinctly by 20 cm⁻¹ to lower energy upon triazolylidene coordination ($\nu_{\text{CO}} = 2018, 1967 \text{ cm}^{-1}$ in **2**, and 1999, 1938 cm⁻¹ in **3b**, Table 1). The bathochromic shift is slightly but consistently more pronounced when the triazolylidene ligand contained only alkyl substituents, and less strong when phenyl substituents are present, irrespective of the connectivity pattern. The carbene ligand in **3a** with the phenyl group attached to the carbon induced the same shift as the analogous carbene with the phenyl group attached to nitrogen (**3d**). These data suggest that the CO stretch vibration may be used as a probe for the qualitative assessment of the carbene donor properties.^{23,24} In line with this notion, coordination of 2-imidazolylidenes induces a slightly smaller bathochromic shift ($\Delta\nu = 4 \text{ cm}^{-1}$), which reflects their weaker donor properties when compared to triazolylidenes.^{20a,b} Potentially, backbonding from the electron-rich ruthenium(0) center to the carbene ligand may affect the CO stretch vibration and may thus complicate a simple linear correlation between IR frequencies and donor properties.

Table 1. Relevant carbonyl stretch vibrations (cm^{-1}) of the complexes

| complex | Ru–CO | Cp=O |
|----------------------------|------------|------|
| 2 | 2018, 1967 | --- |
| 3a | 2004, 1945 | 1577 |
| 3b | 1999, 1938 | 1583 |
| 3c | 1998, 1937 | 1584 |
| 3d | 2003, 1944 | 1578 |
| 3a + HBF_4 | 2036, 1979 | --- |

Further evidence of the formation of complexes **3a–d** was obtained from NMR data, in particular the disappearance of the low field signal of the triazolium precursor in the ^1H NMR spectrum and the downfield shift of the carbenic resonance in the ^{13}C NMR spectra. This nucleus resonates in the 154–158 ppm range and hence some 20 ppm higher field than in ruthenium(II) complexes, indicative for a low valent and electron-rich metal center.

Unambiguous structural evidence was obtained by X-ray diffraction analysis of single crystals of complexes **3a** and **3d**. The molecular structure reveals the expected piano-stool geometry with the cyclopentadienone ligand occupying one face and the two CO ligands and the triazolylidene forming the three legs (Fig. 1). Bond lengths and angles (Table 2) are very similar in both complexes, suggesting only marginal steric consequences upon swapping the methyl and phenyl wingtip groups in the triazolylidene ligand. As expected, the Ru– C_{trz} bond is longer in complexes **3a** and **3d** than in analogues featuring a higher-valent ruthenium(II) metal center ($\Delta d = 0.06 \text{ \AA}$).¹⁵

Table 2. Selected bond lengths (\AA) and angles (deg) for complexes **3a** and **3d**.

| | 3a | 3d |
|-------------------------|------------|-----------|
| Ru–C1 | 2.1196(12) | 2.120(2) |
| Ru–C42 | 1.8965(13) | 1.878(2) |
| Ru–C43 | 1.8825(13) | 1.898(2) |
| Ru–Cg ^{a)} | 1.930(<1) | 1.932(<1) |
| C1–Ru–C42 | 95.18(5) | 91.08(8) |
| C1–Ru–C43 | 91.66(6) | 95.90(8) |
| C1–Ru–Cg ^{a)} | 116.44(3) | 115.02(5) |
| C42–Ru–Cg ^{a)} | 125.76(4) | 125.60(7) |
| C43–Ru–Cg ^{a)} | 127.83(4) | 127.44(6) |
| C42–Ru–C43 | 90.99(6) | 92.96(9) |
| C11–O1 | 1.2464(14) | 1.239(2) |

a) Cg = centroid of cyclopentadienone ligand

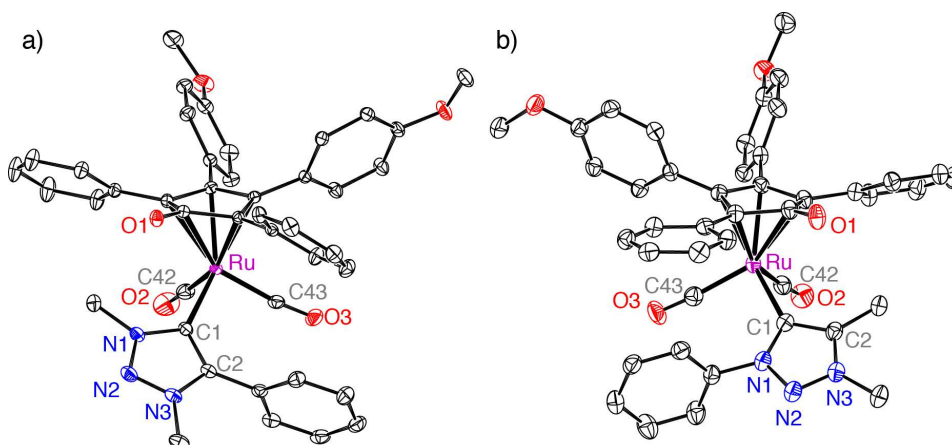


Figure 1. ORTEP representations (50% probability level, hydrogen atoms omitted for clarity) of complexes **3a** (a) and **3d** (b).

Catalytic alcohol oxidation

The triazolylidene Ru(0) complex **3a** was evaluated as catalyst precursor for the oxidation of alcohols using benzyl alcohol (BnOH) as model substrate. While ruthenium(II) systems with a cymene spectator ligand gave attractive conversions even in the absence of oxidants or base,¹⁵ runs performed with **3a** in the absence of such additives were essentially non-productive with <5% conversion (Table 3, entry 1). Better results were obtained upon adding $[\text{Ce}(\text{NH}_3)_6](\text{NO}_3)_2$ (CAN) as oxidizing agent to activate the catalyst precursor **3a**.²⁵

Table 3. Ruthenium/cerium-catalyzed BnOH oxidation^{a)}

| Entry | Ru ⁰ complex | mol% Ce ^{IV} | yield (2 h) | yield 24 h |
|-------|-------------------------|-----------------------|-------------|-------------------|
| 1 | 3a | --- | <5% | <5% |
| 2 | --- | 10 | 25% | 80% |
| 3 | --- | 5 | 12% | 42% |
| 4 | --- | 2.5 | 12% | 31% |
| 5 | 3a | 10 | 57% | 97% ^{b)} |
| 6 | 3a | 5 | 24% | 85% |
| 7 | 3a | 2.5 | 20% | 84% |
| 8 | 2 | 10 | 19% | 81% |

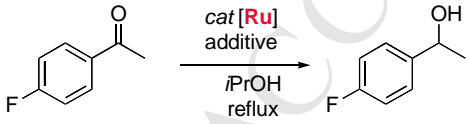
a) General conditions: 0.19 mmol BnOH, 5 mol% Ru⁰ complex, 3 mL 1,2-C₆H₄Cl₂, mol% Ce^{IV} and Ru relative to BnOH; 150 °C, yield of PhCHO determined by ¹H NMR spectroscopy by using anisole as internal standard; b) reaction complete after 8 h.

Initial background measurements indicated that in the absence of a ruthenium complex, CAN catalyzes the oxidation of BnOH to benzaldehyde on its own under the applied reaction conditions. Background conversions reached 80% when 10 mol% CAN was used, and dropped to 40% and 30% approximately, if the CAN loading was reduced to 5 and 2.5 mol%, respectively (entries 2–4, Fig. S1–S3). Addition of complex **2**, *i.e.* the carbene-free ruthenium(0) precursor, had no notable effect and yields and conversions mirrored those of CAN only (entry 8). Possibly, the lack of a stabilizing ligand for ruthenium(II) induces rapid decomposition, supported also by the brown color that rapidly developed upon heating the mixture. In contrast, complex **3a** induced a considerable acceleration (entries 5–7). For example, with 5 mol% **3a** and 2.5 mol% CAN, 84% conversion was accomplished within 24 h (*cf.* 31% conversion in the background reaction). At higher CAN loading (10 mol%), the catalytic competence of **3a** is evident in particular at early stages of the oxidation. After 2 h, 57% conversion was observed with the Ru⁰/Ce^{IV} couple (25% with Ce^{IV} only, 0% with Ru⁰ only), and oxidation was essentially complete after less than 8 h. While the selectivity is typically high and conversion occurs selectively to the desired aldehyde, further improvement of the catalytic performance of **3a** may need a focus on an oxidant for ruthenium that is less catalytically active than CAN.

Catalytic transfer hydrogenation

In addition to alcohol dehydrogenation, we were also interested to see whether complexes **3** are active in transfer hydrogenation. A model reaction employed complex **3a** as catalyst precursor and 4-fluoroacetophenone as substrate under standard transfer hydrogenation conditions,²⁶ *i.e.* refluxing *i*PrOH as hydrogen source (Table 4).

Table 4. Catalytic transfer hydrogenation of 4-fluoroacetophenone ^{a)}



| entry | Ru ⁰ complex | additive ^{b)} | yield (%) 8h | yield (%) 24h |
|-------|-------------------------|------------------------|--------------|--------------------|
| 1 | 3a | --- | 0 | <5 |
| 2 | 2 | --- | 96 | n.d. ^{c)} |
| 3 | 3a | KOH | 0 | 6 |
| 4 | 2 | KOH | 95 | n.d. ^{c)} |
| 5 | 3a | HBF ₄ | <5 | 31 |
| 6 | 2 | HBF ₄ | 55 | 59 |
| 7 | 3a | CAN | 59 | 89 |
| 8 | 2 | CAN | 0 | 7 |
| 9 | 3a | CAN + HBF ₄ | 42 | 44 |
| 10 | 3a | CAN + KOH | 6 | 17 |

a) General conditions: Ruthenium complex (5 mol% Ru), *i*PrOH (5 mL), reflux; yield of alcohol determined by ^1H NMR spectroscopy; b) quantities of additives as follows: HBF_4 1 molequiv., KOH 2 molequiv., CAN 1 molequiv. per ruthenium center; c) n.d. = not determined due to complete conversion after 8 h.

Catalytic runs were performed in particular for comparing the catalytic activity of the triazolylidene ruthenium(0) complex **3a** and the triazolylidene-free dimeric precursor **2** under various conditions.²⁵ In the absence of any additives (entries 1,2), complex **3a** is inactive and essentially no conversion was observed, while precursor **2** reaches almost complete conversion within 8 h in pure *i*PrOH. Addition of KOH did not change the relative performance and conversions were identical to those in *i*PrOH only (entries 3,4). These results suggest that KOH is not a suitable additive for the activation of the ruthenium center in complex **3a**, probably because the electron-rich ruthenium(0) center has no affinity for binding a hard alkoxide ligand, nor for dissociation of a CO ligand due to the high donor properties of the triazolylidene ligand, which are assumed to enhance Ru-CO backbonding. Conversely, the activity observed for complex **2** probably arises from splitting of the dimeric precursor into two monomeric forms which, in the presence of a hydrogen source lead to a derivative of Shvo's catalyst (**A**, Figure 2).²² Such complexes are well-known to catalyze the transfer hydrogenation of a broad range of ketones.²²

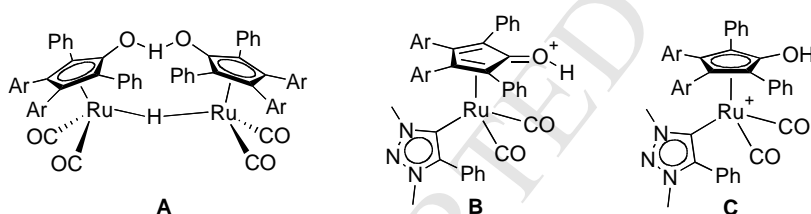


Figure 2. Shvo-type catalyst **A** resulting from cleavage of dimer **2** in *i*PrOH, and cationic complexes **B** and **C** from protonation of complex **3a**, featuring a ruthenium(0) and a ruthenium(II) center, respectively.

In an attempt to labilize the CO ligands, a proton source was introduced. Protonation at the dienone system has been reported and may provide a cationic structure with a positive charge either at the oxygen (complex **B**, Fig. 2) or at the ruthenium center (**C**), thus inducing formal oxidation of the metal center to ruthenium(II) and depletion of electron density, which in turn is expected to substantially reduce the π character of the Ru-CO bond. Stoichiometric experiments using HCl (10 molequiv.) or HBF_4 (5 molequiv.) in CH_2Cl_2 with complex **3a** indeed gave cationic complexes in which the carbonyl stretch vibration was significantly shifted to higher frequency ($\nu_{\text{CO}} = 2036$ and 1979 cm^{-1} , cf. 2004 cm^{-1} , 1945 cm^{-1} in **3a**), and the ketone C=O vibration observed in **3a** for the

Cp=O ligand disappeared in the cationic complexes. These data strongly suggesting formation of a cyclopentadienyl-type ligand as in complex **C**. Transfer hydrogenation in the presence of HBF₄ (1 equiv) did indeed increase the catalytic activity of complex **3** (entry 5), however the 30% conversion after 24 h is unremarkable when compared with other ruthenium carbene systems.²⁷ The dimeric complex **2** performs significantly less in the presence of acid (entry 6), in agreement with the formation of a Shvo-type active system from formal dihydrogen transfer rather than protonation. Best result for complex **3a** were obtained when using CAN as an oxidizing agent. Under these conditions, oxidation of the metal center from ruthenium(0) to ruthenium(II) takes place (see below), which weakens the bonding of CO and hence produces a methodology to activate the complex. In the presence of CAN, conversion of 4-fluoroacetophenone reaches 58% after 8 h and 89% after 24 h (entry 7). In contrast, CAN efficiently quenches the activity of complex **2** (entry 8). Hence, conditions have been developed that favor catalytic transfer hydrogenation using the dimer **2** but not **3a** (entries 1,2), and inversely, conditions that favor activity of complex **3a** but not **2** (entries 7,8). These results demonstrate the orthogonality induced upon bonding of a triazolylidene ligand. Addition of either base or acid to the CAN-activated complex **3a** are not advantageous and conversions were consistently lower (entries 9,10). Variation of the amount of CAN did not result in further enhancement of activity. Both lowering the amount to 0.25 or 0.5 equiv relative to **3a** as well as increasing the amount to 2, 4 or 6 equivalents resulted in slower and generally incomplete conversion (Fig. S4). In particular using excess CAN lead to substantial catalyst deactivation after around 5 h.

Electrochemical measurement

Electrochemical analysis of the triazolylidene ruthenium(0) complex **3a** by cyclic voltammetry measurements reveal a quasi-reversible oxidation of **3a** in CH₂Cl₂ solution with $E_{1/2} = +0.952(\pm 3)$ vs SCE (Fig. 3, Fig. S5). The redox process likely involves a Ru⁰/Ru^I oxidation which is according to the peak-current ratio reversible at higher scan rates ($i_{pc}/i_{pa} = 0.96$ at 200 mV s⁻¹) and less reversible at slower scan rates ($i_{pc}/i_{pa} = 0.56$ at 20 mV s⁻¹), suggesting a slow chemical transformation of the oxidized species (EC mechanism).²⁸ The i_{pc}/i_{pa} ratio at different scan rates fits excellently with an irreversible first-order reaction after the oxidation process, with a rate constant $k = 0.58$ s⁻¹ for the homogeneous follow-up reaction (correlation > 0.99, Table S1, Fig. S6). These data are in agreement with a metal-centered oxidation process and subsequent slow dissociation of CO from the coordination sphere due to the lower electron-density upon ruthenium oxidation (*cf.* CAN-mediated activity of **3a** in transfer hydrogenation). Consistent with this model,

electrochemical analysis of **3a** measured in MeCN shows a largely irreversible oxidation process ($E_{pa} = +0.96$ V, $i_{pc}/i_{pa} = 0.64$) even at high scan rates (500 mV s⁻¹; Fig. S7). The coordinating properties of MeCN may thus accelerate the substitution of CO and thus the EC mechanism.

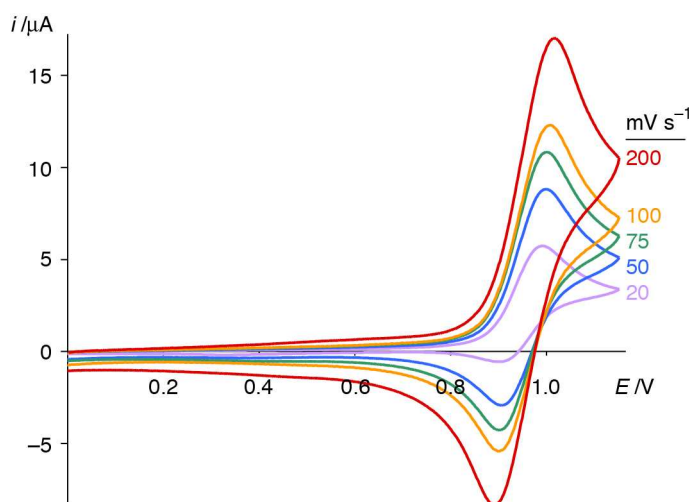


Figure 3. Cyclic voltammograms for **3a** in CH₂Cl₂ at different scan rates (potential vs SCE, Fc as internal standard).

Since the catalytic activity of the ruthenium complex **3a** was considerably enhanced when pre-activated with CAN, both for transfer hydrogenation and alcohol dehydrogenation, a series of electrochemical measurements was performed on **3a** in the presence of CAN. When 0.5 molequiv CAN were added to a solution of **3a** in MeCN, differential pulse voltammetry revealed three oxidation processes (Fig. 4). The first process at $E = +0.90$ V pertains to the Ru⁰/Ru^I oxidation of complex **3a** and was also observed in measurements without CAN,²⁹ and the second process with $E = +1.06$ V corresponds to a cerium-centered oxidation.³⁰ A third oxidation process at $E = +1.22$ V with equal ratio to the first process is assumed to belong to a new species resulting from oxidation of complex **3a** and has thus tentatively been attributed to a Ru^I/Ru^{II} oxidation. The equal relative intensities of the first and last oxidation processes remain constant over several hours, suggesting an equilibrium. The 1:1 ratio indicates equal quantities of two ruthenium species, which agrees well with the provision of 0.5 molequiv CAN at the onset of the experiment and suggests a complete one-electron transfer from ruthenium(0) to cerium(IV), thus resulting in 50% [**3a**]⁺ and 50% of the parent complex **3a**. In support of such a model, no oxidation process at +0.9 V was detected after addition of 1 molequiv CAN, thus indicating the absence of significant amounts of the original complex **3a**. Instead, only an oxidation process at $E = +1.22$ V was detected, together with the cerium-centered oxidation. These measurements are thus consistent with a CAN-mediated oxidation of the ruthenium-center in **3a** to ruthenium(II) by consumption of two equivalents of cerium(IV),

and concomitant release of CO (EC mechanism) as a process for entering the catalytic cycle. Such processes require the presence of a stabilizing donor ligand such as the triazolylidene used in this study.

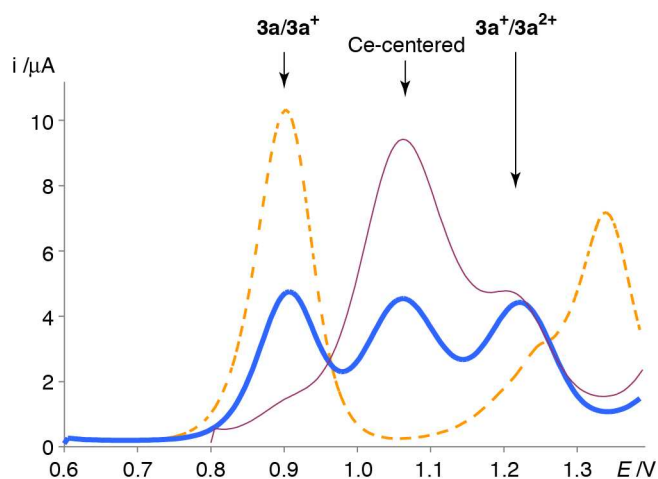


Figure 4. Relevant section of differential pulse voltammetry analysis of complex **3a** in presence of different equivalent of CAN: 0 equiv (orange dashed line), 0.5 equiv (blue bold line) and 1.0 equiv (red thin line; all measurements in MeCN at 50 mV s^{-1} , potential vs SCE, Fc as internal standard).

Conclusions

A set of ruthenium(0) complexes **3** has been prepared which contain differently substituted triazolylidene ligands, thus demonstrating the suitability of such strongly donating NHC ligands to stabilize low-valent metal centers. Catalytic activity in hydrogen transfer reactions has been evidenced, though oxidative activation with CAN as a potent auxiliary is required. For alcohol dehydrogenation, both CAN and the ruthenium complex are pre-catalysts and the relative quantities of the two components can be used to increase the relevance of either the Ce- or the Ru-catalyzed transformation. Detailed electrochemical analyses lend support to a fast two-step oxidation of the ruthenium center of **3** in order to enter the catalytic cycle, an activation process that is complementary to that of the dimeric ruthenium carbonyl complex **2**. Upon addition of a triazolylidene ligand, loss of CO appears to be essential for the generation of an open coordination site for substrate coordination and catalytic turnover. Triazolylidene ligands with their strongly mesoionic character may be particularly useful for facilitating the metal oxidation and for entailing such catalyst activation. This concept may become particularly useful when employing other low-

valent complexes as catalyst precursors and may provide an interesting opportunity for exploiting base metals in catalysis.

Experimental Section

General comments. The syntheses of the ruthenium complexes were carried out under an inert atmosphere of N₂ using Schlenk techniques and dry solvents. Purifications were performed in air using commercial solvents. ¹H and ¹³C{¹H} NMR spectra were recorded at room temperature on Varian spectrometers operating at 400 or 500 MHz unless stated otherwise. Chemical shifts (δ in ppm, J in Hz) were referenced to SiMe₄. Signal assignments are based on homo- and heteronuclear (multiple-bond) correlation spectroscopy. Elemental analyses were performed by the Microanalytical Laboratory at the University College Dublin, Ireland. Infra-red spectra were recorded on a Perkin Elmer FTIR at 1 cm⁻¹ resolution. Electrochemical studies were carried out on a Metrohm Autolab PGSTAT101 potentiostat using a gas-tight three electrode cell under an argon atmosphere. A platinum disk with 3.8 mm² surface area was used as the working electrode and was polished before each measurement. The reference electrode was Ag/AgCl, the counter electrode was a Pt wire. In all experiments, [Bu₄N]PF₆ (100 mM in dry CH₂Cl₂ or MeCN) was used as supporting electrolyte with analyte concentrations of approximately 1 mM. The redox potentials were referenced to ferrocenium/ferrocene (Fc⁺/Fc; $E_{1/2} = 0.46$ V vs. SCE in CH₂Cl₂; $E_{1/2} = 0.40$ V vs. SCE in MeCN).³¹ The ruthenium precursors **2**¹⁹ and the triazolium salts **1a-d** were prepared according to literature procedures.¹⁵ All other reagents were purchased from commercial sources and were used as received, unless otherwise stated.

General procedure for the synthesis of the ruthenium complexes 3. The triazolium salts **1a-d** were reacted at room temperature with Ag₂O (0.5 eq.) in CH₂Cl₂ solution under inert atmosphere and protected from light. After 2 h, the dimeric ruthenium precursor **2** (0.5 eq.) was added to the mixture and stirring continued for 2 h. The mixture was then filtered through a short pad of Celite and filtrate was evaporated to yield the triazolylidene Ru(0) complexes **3a-d** in typically quantitative yield. Suitable crystals for X-Ray diffraction were obtained by slow diffusion of pentane into a CH₂Cl₂ solution of the complex.

Analytical data for dicarbonyl-(η^4 -3,4-bis(4-methoxyphenyl)-2,5-diphenylcyclopenta-2,4-dienone)(1,3-dimethyl-4-phenyl-1,2,3-triazol-ylidene)ruthenium (3a).

^1H NMR (300 MHz, CD_2Cl_2): δ = 7.59–7.51 (m, 4H, CH_{aryl}), 7.32–7.01 (m, 15H, CH_{aryl} + CH_{Ph}), 6.58–6.50 (m, 4H, CH_{aryl}), 3.63 (s, 6H, OCH_3), 3.61, 3.56 (2 \times s, 3H, NCH_3); $^{13}\text{C}\{^1\text{H}\}$ NMR (400 MHz, CD_2Cl_2): δ = 203.11 (Ru–CO), 169.08 ($\text{C}_{\text{Cp}}=\text{O}$), 159.31 (COMe), 157.57 (Ru– C_{trz}), 150.38 ($\text{C}_{\text{trz}}-\text{Ph}$), 136.51 ($\text{C}_{\text{aryl}}-\text{Cp}$), 134.45 (CH_{aryl}), 131.83, 130.48, 129.33 (3 \times C_{Ph}), 128.46 (CH_{aryl}), 128.19 (CH_{aryl}), 125.93 (C_{aryl}), 124.90 (CH_{aryl}), 113.34 (CH_{aryl}), 103.91 ($\text{C}_{2,5}$ Cp), 80.59 ($\text{C}_{3,4}$ Cp), 55.77 (OCH_3), 42.11, 37.48 (2 \times NCH_3). IR (CH_2Cl_2) ν_{CO} : 2004 cm^{-1} , 1945 cm^{-1} , 1577 cm^{-1} . ESI-MS (m/z) = 776 [$\text{M}+\text{H}$] $^+$; 798 [$\text{M}+\text{Na}$] $^+$. Anal. Calcd (%) for $\text{C}_{43}\text{H}_{35}\text{N}_3\text{O}_5\text{Ru}$ (774.82): C, 66.66; H, 4.55; N 5.42. Found: C, 65.95; H, 4.64; N 5.34.

Analytical data for dicarbonyl-(η^4 -3,4-bis(4-methoxyphenyl)-2,5-diphenylcyclopenta-2,4-dienone)(1,4-dibutyl-3-methyl-1,2,3-triazolylidene)ruthenium (3b).

^1H NMR (300 MHz, CDCl_3): δ = 7.8–7.2 (m, 4H, CH_{aryl}), 7.37–6.63 (m, 10H, CH_{aryl}), 6.62–6.50 (m, 4H, CH_{aryl}), 3.81 (s, 3H, NCH_3), 3.63 (s, 6H, OCH_3), 3.61 (m, 2H, NCH_2), 1.87–1.03 (m, 10H, – CH_2 –), 0.73 (m, 6H, CH_2CH_3). $^{13}\text{C}\{^1\text{H}\}$ NMR (400 MHz, CDCl_3): δ = 202.90 (CO), 158.44 (COMe), 154.01 (Ru– C_{trz}), 148.55 ($\text{C}_{\text{trz}}-\text{Bu}$), 135.59 (C_{aryl}), 133.71 (CH_{aryl}), 129.11 (CH_{aryl}), 127.37 (CH), 125.25 (C_{aryl}), 125.06 (CH_{aryl}), 112.87 (CH_{aryl}), 103.85 ($\text{C}_{2,5}$ Cp), 78.43 ($\text{C}_{3,4}$ Cp), 55.02 (OCH_3), 53.31 (NCH_2), 36.05 (NCH_3), 32.08 (NCH_2CH_2), 31.24 ($\text{C}_{\text{trz}}-\text{CH}_2$), 23.55 ($\text{C}_{\text{trz}}-\text{CH}_2\text{CH}_2$), 22.38, 19.39 (2 \times CH_2CH_3), 14.05, 13.60 (2 \times CH_2CH_3). IR (CH_2Cl_2) ν_{CO} : 1999 cm^{-1} , 1938 cm^{-1} , 1583 cm^{-1} .

Analytical data for dicarbonyl-(η^4 -3,4-bis(4-methoxyphenyl)-2,5-diphenylcyclopenta-2,4-dienone)(1,3,4-tributyl-1,2,3-triazolylidene)ruthenium (3c).

^1H NMR (300 MHz, CD_2Cl_2): δ = 7.78–7.64 (m, 4H, CH_{aryl}), 7.21–7.03 (m, 10H, CH_{aryl}), 6.69–6.61 (m, 4H, CH_{aryl}), 4.10–3.98 (m, 2H, NCH_2), 3.70 (s, 6H, OCH_3), 3.70–3.58 (m, 2H, NCH_2), 1.79–1.04 (m, 14H, CH_2 Bu), 0.95–0.67 (m, 9H, CH_2CH_3); $^{13}\text{C}\{^1\text{H}\}$ NMR (400 MHz, CD_2Cl_2): δ = 204.09 (CO), 169.47 ($\text{C}_{\text{Cp}}=\text{O}$), 159.45 (COMe), 157.58 (Ru– C_{trz}), 148.96 ($\text{C}_{\text{trz}}-\text{Bu}$), 136.81 (C_{aryl}), 134.60 (CH_{aryl}), 129.90 (CH_{aryl}), 128.10 (CH), 126.36 (C_{aryl}), 125.80 (CH_{aryl}), 113.56 (CH_{aryl}), 104.48 ($\text{C}_{2,5}$ Cp), 79.07 ($\text{C}_{3,4}$ Cp), 55.82 (OCH_3), 50.13 (NCH_2), 34.96 (NCH_3), 32.77, 32.67 (2 \times NCH_2CH_2), 32.19 ($\text{C}_{\text{trz}}-\text{CH}_2$), 24.28 ($\text{C}_{\text{trz}}-\text{CH}_2\text{CH}_2$), 23.18, 20.36, 20.17 (3 \times CH_2CH_3), 14.63, 14.14, 14.09 (3 \times CH_2CH_3). IR (CH_2Cl_2) ν_{CO} : 1998 cm^{-1} , 1937 cm^{-1} , 1584 cm^{-1} .

Analytical data for dicarbonyl-(η^4 -3,4-bis(4-methoxyphenyl)-2,5-diphenylcyclopenta-2,4-dienone)(1-phenyl-3,4-dimethyl-1,2,3-triazol-ylidene)ruthenium (3d**).**

^1H NMR (300 MHz, CDCl_3) δ (ppm): 7.59–7.49 (m, 4H, CH_{aryl}), 7.28–6.92 (m, 15H, CH_{aryl} + CH_{Ph}), 6.64–6.55 (m, 4H, CH_{aryl}), 3.87 (s, 3H, NCH_3), 3.66 (s, 6H, OCH_3), 1.79 (s, 3H, $\text{C}_{\text{trz}}\text{-CH}_3$); $^{13}\text{C}\{^1\text{H}\}$ NMR (400 MHz, CDCl_3): δ = 202.41 (CO), 167.75 ($\text{C}_{\text{Cp}}=\text{O}$), 159.84 (Ru– C_{trz}), 158.27 (COMe), 145.38 ($\text{C}_{\text{trz}}\text{-Me}$), 139.18 (C_{aryl}), 135.45–112.64 (C_{aryl}), 133.57, 129.54, 127.31 ($3 \times \text{C}_{\text{Ph}}$), 103.34 ($\text{C}_{2,5 \text{ Cp}}$), 79.72 ($\text{C}_{3,4 \text{ Cp}}$), 54.95 (OCH_3), 35.99 (NCH_3), 10.53 (trz-CH_3). ESI-MS (m/z): 798 [$\text{M}+\text{Na}$] $^+$. IR (CH_2Cl_2) ν_{CO} : 2003 cm^{-1} , 1944 cm^{-1} , 1578 cm^{-1} .

General condition for alcohol oxidation: Complex **3a** (7.4 mg, 9.5 μmol , 5 mol%), 1,2-dichlorobenzene (3 mL), and the appropriate amount of $[\text{Ce}(\text{NH}_3)_6](\text{NO}_3)_2$ dissolved in MeCN (0.5 mL) were stirred at reflux for 15 min. Benzyl alcohol (20 μL , 190 μmol) was then added. Aliquotes (0.05 mL) were taken from the mixture at selected intervals, diluted with CDCl_3 (0.5 mL) and conversions were determined by ^1H NMR spectroscopy.

General conditions for transfer hydrogenation: Complex **3a** (12 mg, 15 μmol , 5 mol%), CAN (8 mg, 15 μmol , 5 mol%) and *i*PrOH (5 mL) were stirred at reflux for 15 min. Then 4-fluoroacetophenone (36 μL , 300 μmol) was added and samples were taken at regular intervals. Aliquots (ca. 0.05 mL) were diluted with CDCl_3 (0.5 mL) and conversions were determined by ^1H NMR spectroscopy.

Crystallographic details. Crystal data for complexes **3a** and **3d** were collected by using an Agilent Technologies SuperNova A diffractometer fitted with an Atlas detector using Mo- K_α radiation (0.71073 Å; **3a**) or Cu- K_α radiation (1.54184 Å; **3d**). A complete dataset was collected, assuming that the Friedel pairs are not equivalent. An analytical numeric absorption correction was performed.³² The structure was solved by direct methods using SHELXS-97³³ and refined by full-matrix least-squares fitting on F^2 for all data using SHELXL-97.³³ Hydrogen atoms were added at calculated positions and refined by using a riding model. Their isotropic temperature factors were fixed to 1.2 times (1.5 times for methyl groups) the equivalent isotropic displacement parameters of the carbon atom the H-atom is attached to. Anisotropic thermal displacement parameters were used for all nonhydrogen atoms. Crystallographic details are compiled in the supporting information (Table S2).

Acknowledgements

Financial support for this work is acknowledged from Science Foundation Ireland through the Synthesis and Solid State Pharmaceutical Center (SSPC), by the European Research Council (ERC CoG 615653) and the Marco Polo scheme of the University of Bologna for supporting an exchange visit to CC.

Appendix A. Supplementary material

Time-conversion profiles for catalytic reactions, electrochemical data, and crystallographic details. CCDC number 1043258 and 1043259 contain the supplementary crystallographic data for this paper. These data can be obtained free of charge from the Cambridge Crystallographic Data Centre via www.ccdc.cam.ac.uk/data_request/cif.

References

- [1] For selected reviews, see: a) D. Bourissou, O. Guerret, F. P. Gabbai, G. Bertrand, *Chem. Rev.* 100 (2000) 39; b) W. A. Herrmann, *Angew. Chem. Int. Ed.* 41 (2002) 1290; c) C. M. Crudden, D. P. Allen, *Coord. Chem. Rev.* 248 (2004) 2247; d) M. Poyatos, J. A. Mata, E. Peris, *Chem. Rev.* 109 (2009) 3677; e) O. Schuster, L. Yang, H. G. Raubenheimer, M. Albrecht, *Chem. Rev.* 109 (2009) 3445; f) L. Mercks, M. Albrecht, *Chem. Soc. Rev.* 39 (2010) 1903; g) S. P. Nolan, *N-heterocyclic carbenes*, Wiley-VCH, Weinheim (Germany) 2014.
- [2] For reviews, see: a) F. E. Hahn, M. C. Jahnke, *Angew. Chem. Int. Ed.* 47 (2008) 3122; b) M. Melaimi, M. Soleilhavoup, G. Bertrand, *Angew. Chem. Int. Ed.* 49 (2010) 8810. c) L. Benhamou, E. Chardon, G. Lavigne, S. Bellemin-Laponnaz, V. Cesar, *Chem. Rev.* 111 (2011) 2705. d) L. A. Schaper, S. J. Hock, W. A. Herrmann, F. E. Kühn, *Angew. Chem. Int. Ed.* 52 (2013) 270.
- [3] a) C. Samojłowicz, M. Bieniek, K. Grela, *Chem. Rev.* 109 (2009) 3708; b) S. Monfette, D. E. Fogg, *Chem. Rev.* 109 (2009) 3783; c) G. C. Vougioukalakis, R. H. Grubbs, *Chem. Rev.* 110 (2010) 1746.
- [4] a) E. A. B. Kantchev, C. J. O'Brien, M. G. Organ, *Angew. Chem. Int. Ed.* 46 (2007) 2768; b) G. C. Fortman, S. P. Nolan, *Chem. Soc. Rev.* 40 (2011) 5151.

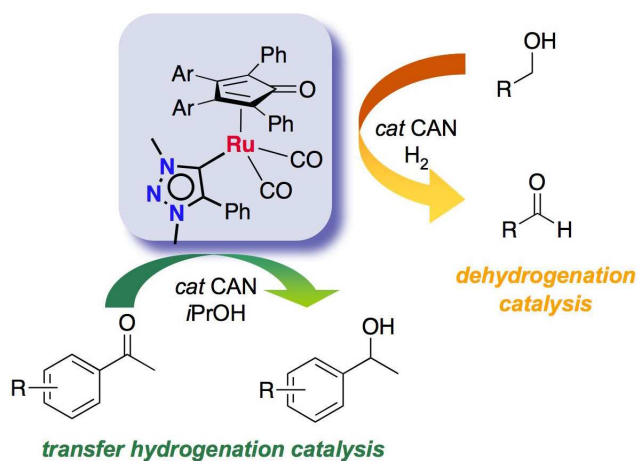
- [5] For examples, see: a) R. Corberan, E. Peris, *Organometallics* 27 (2008) 1954; b) A. Savini, G. Bellachioma, G. Ciancaleoni, C. Zuccaccia, D. Zuccaccia, A. Macchioni, *Chem. Commun.* 46 (2010) 9218; c) A. Petronilho, J. A. Woods, H. Mueller-Bunz, S. Bernhard, M. Albrecht, *Chem. Eur. J.* 20 (2014) 15775.
- [6] a) A. Fürstner, P. W. Davies, *Angew. Chem. Int. Ed.* 46 (2007) 3410; b) N. Marion, S. P. Nolan, *Chem. Soc. Rev.* 37 (2008) 1776; c) A. S. K. Hashmi, *Angew. Chem. Int. Ed.* 47 (2008) 6754.
- [7] a) S. Diez-Gonzalez, N. Marion, S. P. Nolan, *Chem. Rev.* 109 (2009) 3612; b) H. D. Velazquez, F. Verpoort, *Chem. Soc. Rev.* 41 (2012) 7032; c) V. Dragutan, I. Dragutan, L. Delaude, A. Demonceau, *Coord. Chem. Rev.* 251 (2007) 765; d) L. Delaude, A. Demonceau, in *N-heterocyclic carbenes: From Laboratory Curiosities to Efficient Synthetic Tools* (Ed. S. Diez-Gonzalez), RSC Catalysis Series (UK), 2011; e) L. Schwartzburd, M. K. Whittlesey in *N-heterocyclic carbenes* (Ed. S. P. Nolan), Wiley-VCH, Weinheim (Germany) 2014.
- [8] a) J. Witt, A. Pothig, F. E. Kuhn, W. Baratta, *Organometallics* 32 (2013) 4042; b) N. Gurbuz, E. O. Ozcan, I. Ozdemir, B. Cetinkaya, O. Sahin, O. Buyukgungor, *Dalton Trans.* 41 (2012) 2330; c) S. Horn, C. Gandolfi, M. Albrecht, *Eur. J. Inorg. Chem.* (2011) 2863; d) S. Kuwata, T. Ikariya, *Chem. Eur. J.* 17 (2011) 3542; e) H. Ohara, W. W. N. O, A. J. Lough, R. H. Morris, *Dalton Trans.* 41 (2012) 8797; f) W. W. N. O, A. J. Lough, R. H. Morris, *Organometallics* 31 (2012) 2137.
- [9] a) C. Gandolfi, M. Heckenroth, A. Neels, G. Laurenczy, M. Albrecht, *Organometallics* 28 (2009) 5112; b) T. Wang, C. Prankevicius, C. L. Lund, M. J. Sgro, D. W. Stephan, *Organometallics* 32 (2013) 2168; c) B. Bagh, D. W. Stephan *Dalton Trans.* 43 (2014) 15638; via transfer hydrogenation: d) S. Horn, M. Albrecht, *Chem. Commun.* 47 (2011) 8802.
- [10] E. Fogler, E. Balaraman, Y. Ben-David, G. Leitus, L. J. W. Shimon, D. Milstein, *Organometallics* 30 (2011) 3826.
- [11] a) S. Urban, B. Beiring, N. Ortega, D. Paul, F. Glorius, *J. Am. Chem. Soc.* 134 (2012) 1541; b) J. Wysocki, N. Ortega, F. Glorius, *Angew. Chem. Int. Ed.* 53 (2014) 8751.
- [12] B. Kang, Z. Fu, S. H. Hong, *J. Am. Chem. Soc.* 135 (2013) 11704.
- [13] I. S. Makarov, R. Madsen, *J. Org. Chem.* 78 (2013) 6593.

- [14] J. Balogh, A. M. Z. Slawin, S. P. Nolan, *Organometallics* 31 (2012) 3259.
- [15] a) A. Prades, E. Peris, M. Albrecht, *Organometallics* 30 (2011) 1162; b) A. Solvhoj, R. Madsen, *Organometallics* 30 (2011) 6044; c) D. Canseco-Gonzalez, M. Albrecht, *Dalton Trans.* 42 (2013) 7424; d) M. Delgado-Rebollo, D. Canseco-Gonzalez, M. Hollering, H. Müller-Bunz, M. Albrecht, *Dalton Trans.* 43 (2014) 4462; e) B. Bagh, A. M. McKinty, A. J. Lough, D. W. Stephan, *Dalton Trans.* 43 (2014) 12842.
- [16] L. Bernet, R. Larlempuia, W. Ghattas, H. Mueller-Bunz, L. Vigara, A. Llobet, M. Albrecht, *Chem. Commun.* 47 (2011) 8058.
- [17] a) J. A. Cabeza, P. Garcia-Alvarez, *Chem. Soc. Rev.* 40 (2011) 5389; b) J. A. Cabeza, M. Damonte, E. Perez-Carreno, *Organometallics* 31 (2012) 8355; c) J. A. Cabeza, M. Damonte, P. Garcia-Alvarez, E. Perez-Carreno, *Chem. Commun.* 49 (2013) 2813; d) C. E. Ellul, M. F. Mahon, O. Saker, M. K. Whittlesey, *Angew. Chem. Int. Ed.* 46 (2007) 6343; e) L. Benhamou, J. Wolf, V. Cesar, A. Labande, R. Poli, N. Lugan, G. Lavigne, *Organometallics* 28 (2009) 6981.
- [18] C. Cesari, S. Conti, S. Zacchini, V. Zanotti, M. C. Cassani, R. Mazzoni, *Dalton Trans.* 43 (2014) 17240.
- [19] a) C. Cesari, L. Sambri, S. Zacchini, V. Zanotti, R. Mazzoni, *Organometallics* 33 (2014) 2814; b) M. Boiani, A. Baschieri, C. Cesari, R. Mazzoni, S. Stagni, S. Zacchini, L. Sambri, *New. J. Chem.* 36 (2012) 1469.
- [20] a) P. Mathew, A. Neels, M. Albrecht, *J. Am. Chem. Soc.* 130 (2008) 13534; b) K. F. Donnelly, A. Petronilho, M. Albrecht, *Chem. Commun.* 49 (2013) 1145; c) G. Guisado-Barrios, J. Bouffard, B. Donnadieu, G. Bertrand, *Angew. Chem. Int. Ed.* 49 (2010) 4759. For recent applications of triazolyliidenes as ligands, see e.g.: d) J. A. Woods, R. Lalrempuia, A. Petronilho, N. D. McDaniel, H. Müller-Bunz, M. Albrecht, S. Bernhard, *Energy Env. Sci.* 7 (2014) 2316; e) D. Canseco-Gonzalez, A. Petronilho, H. Müller-Bunz, K. Ohmatsu, T. Ooi, M. Albrecht, *J. Am. Chem. Soc.* 135 (2013) 13193.
- [21] a) V. V. Rostovtsev, L. G. Green, V. V. Fokin, K. B. Sharpless, *Angew. Chem. Int. Ed.* 41 (2002) 2596; b) F. Himo, T. Lovell, R. Hilgraf, V. V. Rostovtsev, L. Noodleman, K. B. Sharpless, V. V. Fokin, *J. Am. Chem. Soc.* 127 (2005) 210; c) V. D. Bock, H. Hiemstra, J. H. van Maarseveen, *Eur. J. Org. Chem.* (2006) 51; d) J. E. Moses, A. D. Moorhouse, *Chem. Soc. Rev.* 36 (2007) 1249; e) J. E. Hein, V. V. Fokin, *Chem. Soc. Rev.* 39 (2010) 1302.

- [22] a) Y. Shvo, D. Czarkie, Y. Rahamim, D. F. Chodosh, *J. Am. Chem. Soc.* 108 (1986) 7400; b) M. C. Warner, O. Verho, J.-E. Bäckvall, *J. Am. Chem. Soc.* 133 (2011) 2820; c) B. L. Conley, M. K. Pennington-Boggio, E. Boz, T. J. Williams, *Chem. Rev.* 110 (2010) 2294.
- [23] A. Poulain, D. Canseco-González, R. Hynes-Roche, H. Müller-Bunz, O. Schuster, H. Stoeckli-Evans, A. Neels, M. Albrecht, *Organometallics* 30 (2011) 1021.
- [24] a) A. R. Chianese, X. Li, M. C. Janzen, J. W. Faller, R. H. Crabtree, *Organometallics* 22 (2003) 1663; b) R. A. Kelly, H. Clavier, S. Guidice, N. M. Scott, E. D. Stevens, J. Bordner, I. Samardjiev, C. D. Hoff, L. Cavallo, S. P. Nolan, *Organometallics* 27 (2008) 202.
- [25] See the supporting information for representative time-conversion profiles for the catalytic reactions.
- [26] a) G. Zassinovich, G. Mestroni, S. Gladiali, *Chem. Rev.* 92 (1992), 1051; b) R. Noyori, S. Hashiguchi, *Acc. Chem. Res.* 30 (1997) 97; c) S. Gladiali, E. Alberico, *Chem. Soc. Rev.* 35 (2006) 226; d) J. S. M. Samec, J.-E. Bäckvall, P. G. Andersson, P. Brandt, *Chem. Soc. Rev.* 35 (2006) 237.
- [27] A. Prades, M. Viciano, M. Sanau, E. Peris, *Organometallics* 27 (2008) 4254.
- [28] J. Heinze, *Angew. Chem. Int. Ed. Engl.* 23 (1984) 831.
- [29] A second oxidation process with $E_{pa} = +1.34$ V is probably a consequence of the EC process mentioned above.
- [30] CAN in dry MeCN displays a reversible oxidation at $E_{1/2} = 1.069$ V ($\Delta E = 126$ mV, $i_{pc}/i_{pa} = 0.95$ at 100 mV s⁻¹) see also Fig. S8.
- [31] N.G. Connelly, W.E. Geiger, *Chem. Rev.* 96 (1996) 877.
- [32] R. C. Clark J. S. Reid, *Acta Crystallogr.* A51 (1995) 887.
- [33] G. M. Sheldrick, *Acta Crystallogr.* A64 (2008) 112.

Only for use as graphical abstract entry

Ruthenium(0) complexes containing a strongly donating 1,2,3-triazolylidene ligand were prepared and evaluated as precursors for hydrogen transfer catalysis. Both dehydrogenation and transfer hydrogenation are catalyzed by these complexes when activated with cerium(IV) as oxidant; electrochemical analysis lend support to a ruthenium oxidation process in the catalyst activation step.



Highlights:

- low-valent ruthenium(0) triazolylidene complexes prepared
- catalytic activity in hydrogen transfer reaction upon activation with cerium(IV)
- dehydrogenation and transfer hydrogenation is catalyzed
- catalyst activation process is detailed electrochemically

*Supplementary Material***Ruthenium(0) complexes with triazolylidene spectator ligands: oxidative activation for (de)hydrogenation catalysis**

Cristiana Cesari,^{a,b} Rita Mazzoni,^b Helge Müller-Bunz,^a Martin Albrecht^{*,a}

a) School of Chemistry & Chemical Biology, University College Dublin, Belfield, Dublin 4, Ireland

b) Dipartimento di Chimica Industriale "Toso Montanari", viale Risorgimento 4, 40136 Bologna, Italy

Author contact: E-mail: martin.albrecht@ucd.ie; Fax: +353 17162501

Catalytic time-conversion profiles

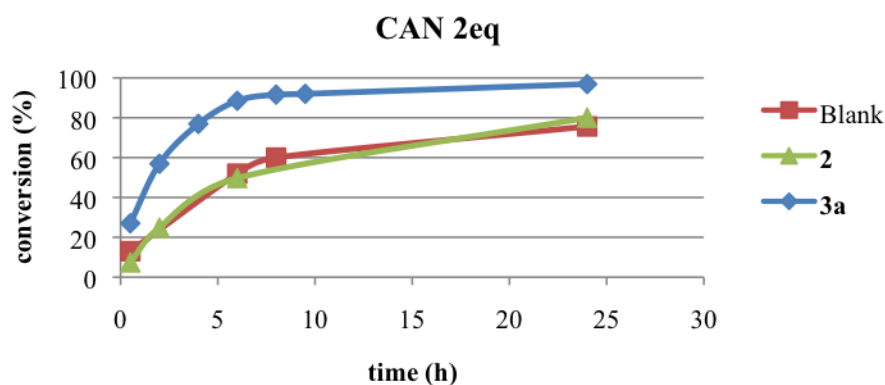


Figure S1. Comparison of conversion for the alcohol oxidation of BnOH with 2 equivalents (per Ru center) of CAN using as pre-catalyst the ruthenium dimer (\blacktriangle), the carbene complex **3a** (\blacklozenge), and the blank without any precursor (\blacksquare)

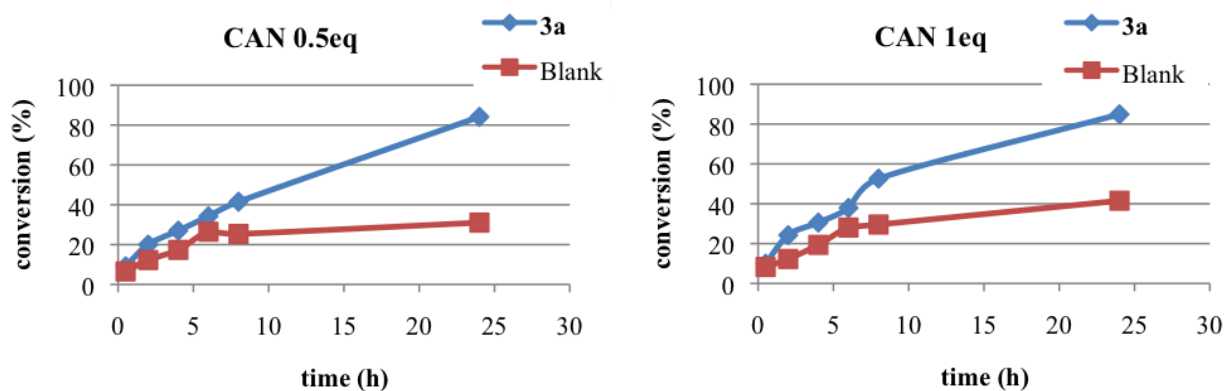


Figure S2. Comparison of conversions for the alcohol oxidation of BnOH with complex **3a** as pre-catalyst (\blacklozenge), and the blank without any precursor (\blacksquare) with 0.5 molequiv CAN (left) and 1 molequiv CAN (right) relative to **3a**.

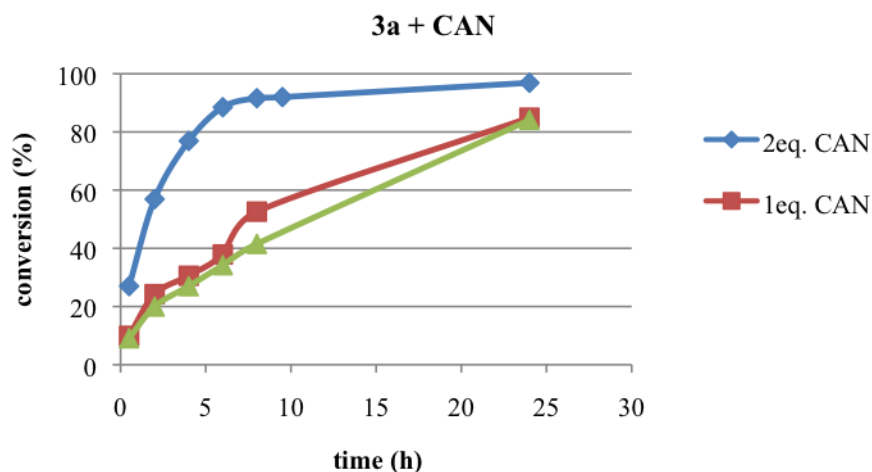


Figure S3. Comparison of conversions for the alcohol oxidation of BnOH with 5 mol% complex **3a** as pre-catalyst with 2 equivalents (\blacklozenge), 1 equivalent (\blacksquare) and 0.5 equivalent (\blacktriangle) of CAN as activator.

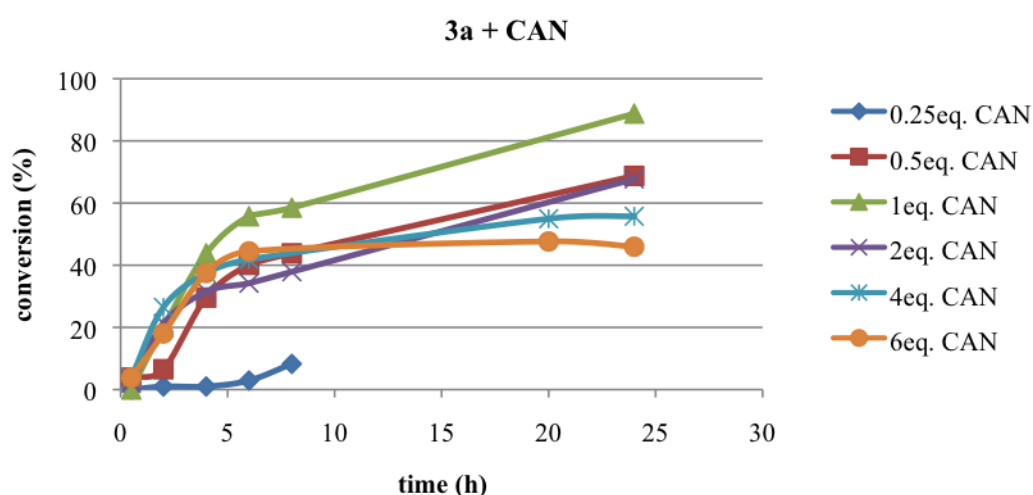


Figure S4. Comparison of the catalytic results for the transfer hydrogenation of 4-fluoroacetophenone with **3a** in the presence of different amounts of CAN. Best results were obtained with stoichiometric quantities of the oxidizing agent; lower amounts of CAN give a lower conversion, probably due to a higher induction time. Higher CAN concentrations induced catalyst deactivation after 4–8 h and gave incomplete conversions. A blank experiment using 10 mol% CAN showed no conversion.

Electrochemical analysis

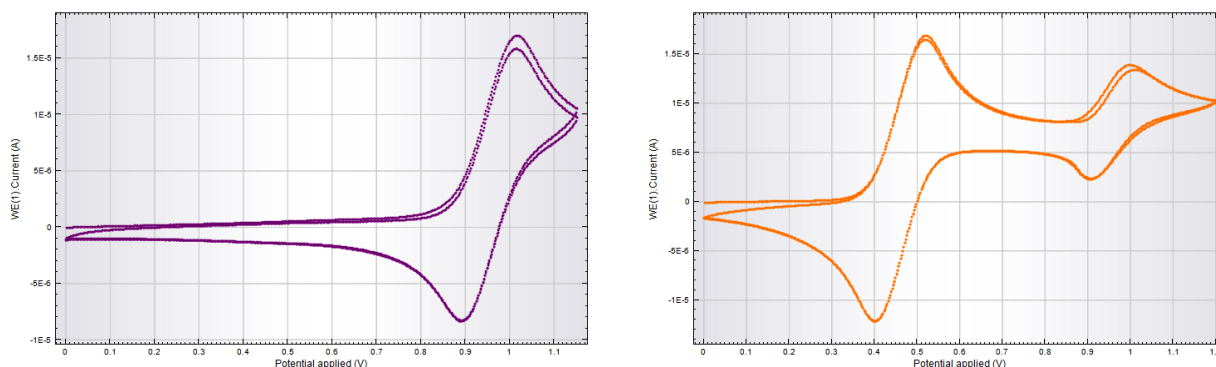


Figure S5. Cyclic Voltammetry of **3a** in CH_2Cl_2 at 200 mV s^{-1} (left) and in the presence of ferrocene (right): $E_{\text{pc}} = 1.013 \text{ V}$ and $E_{\text{pa}} = 0.894 \text{ V}$, hence $E_{1/2} = 0.953 \text{ V}$ ($\Delta E = 120 \text{ mV}$); $i_{\text{pa}} = 17.0 \text{ }\mu\text{A}$ and $i_{\text{pc}} = 16.3 \text{ }\mu\text{A}$, thus $i_{\text{pc}}/i_{\text{pa}} = 0.96$.

Table S1. Scan rate dependence of the +0.95 V oxidation of complex **3a**

| scan rate | $E_{1/2}$ (V) | ΔE (mV) | $i_{\text{pc}}/i_{\text{pa}}$ |
|-------------------------|---------------|-----------------|-------------------------------|
| 20 mV s^{-1} | 0.946 | 90.3 | 0.56 |
| 50 mV s^{-1} | 0.953 | 95.2 | 0.80 |
| 75 mV s^{-1} | 0.954 | 111 | 0.84 |
| 100 mV s^{-1} | 0.956 | 110 | 0.91 |
| 200 mV s^{-1} | 0.953 | 120 | 0.96 |

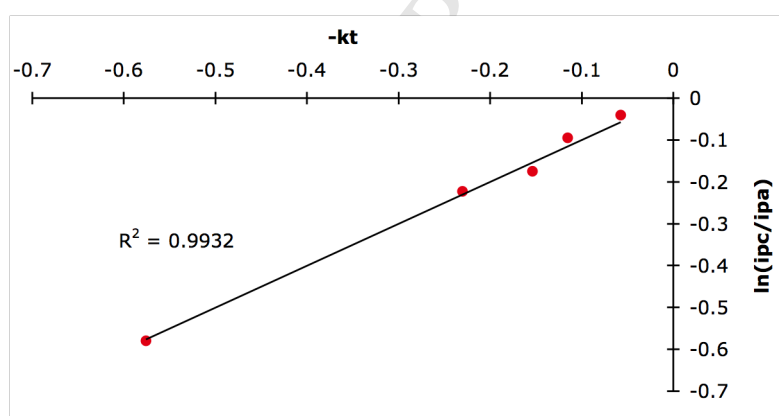


Figure S6. Analysis of $i_{\text{pc}}/i_{\text{pa}}$ ratios at different scan rates provides a linear fit for a coupled first-order irreversible follow-up reaction to the oxidation (EC mechanism) with a first-order rate constant $k = 0.58 \text{ s}^{-1}$ ($t =$ time between passing the $E_{1/2}$ potential and reaching the switching potential E_{max} , here 0.95 V and 1.15 V , respectively).

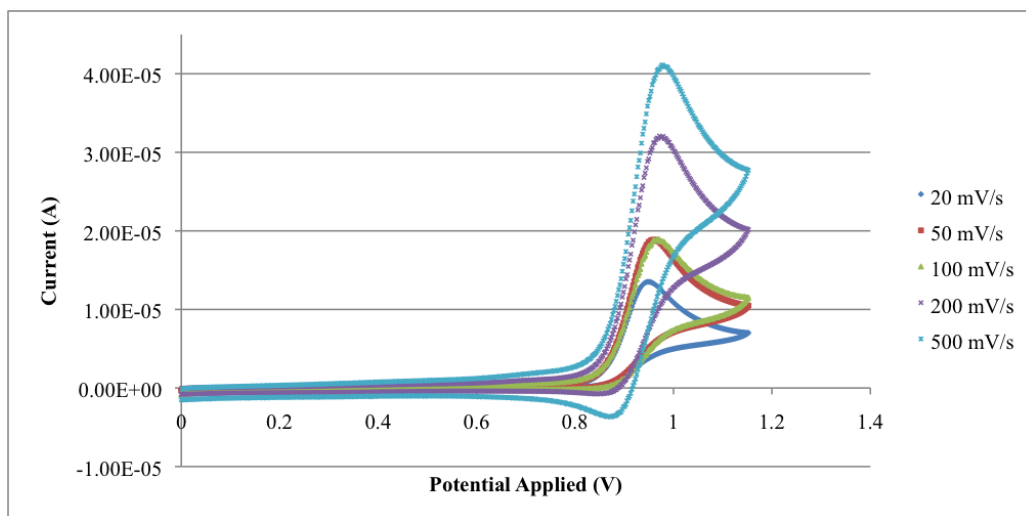


Figure S7. Cyclic Voltammetry diagrams of **3a** in MeCN with different scan rates

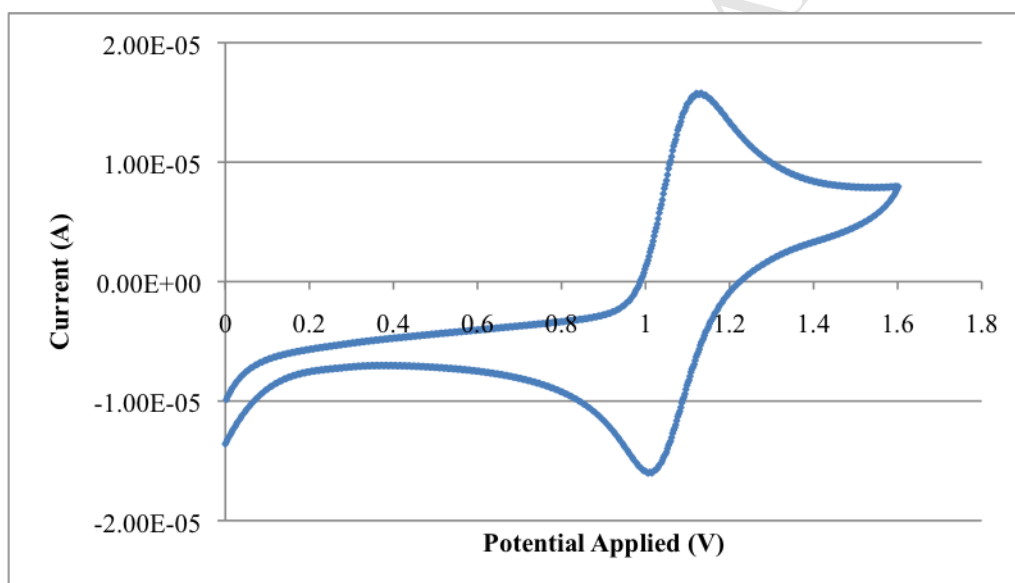


Figure S8. Cyclic voltammogram of CAN measured in MeCN at 100 mV s⁻¹.

*Crystallographic details***Table S2.** Crystallographic details for complexes **3a** and **3d**

| | | |
|-----------------------------------|--|---|
| CCDC No. | 1043258 | 1043259 |
| Empirical formula | C ₄₃ H ₃₅ N ₃ O ₅ Ru | C ₄₃ H ₃₅ N ₃ O ₅ Ru |
| Formula weight | 774.81 | 774.81 |
| Temperature | 100(2) K | 100(2) K |
| Wavelength | 0.71073 Å | 1.54184 Å |
| Crystal system | Monoclinic | Triclinic |
| Space group | P2 ₁ /n (#14) | P-1 (#2) |
| Unit cell dimensions | a = 14.2501(1) Å b = 12.8432(1) Å β = 91.0445(6)° c = 19.6923(2) Å | a = 11.59996(7) Å α = 96.3043(6)° b = 12.4497(1) Å β = 107.6103(6)° c = 13.3559(1) Å γ = 105.4593(6)° |
| Volume | 3603.42(5) Å ³ | 1733.40(2) Å ³ |
| Z | 4 | 2 |
| Density (calculated) | 1.428 Mg m ⁻³ | 1.484 Mg m ⁻³ |
| Absorption coefficient | 0.486 mm ⁻¹ | 4.088 mm ⁻¹ |
| F(000) | 1592 | 796 |
| Crystal size | 0.3520 x 0.2699 x 0.1758 mm ³ | 0.2053 x 0.1485 x 0.0444 mm ³ |
| θ range for data collection | 2.86 to 32.88° | 3.55 to 76.91° |
| Reflections collected | 112232 | 69936 |
| Independent reflections | 12821 [R(int) = 0.0412] | 7272 [R(int) = 0.0366] |
| Completeness to θ = 32.00° | 98.9 % | 99.4 % |
| Absorption correction | Analytical | Analytical |
| Max. and min. transmission | 0.932 and 0.882 | 0.867 and 0.588 |
| Refinement method | Full-matrix least-squares on F ² | Full-matrix least-squares on F ² |
| Data / restraints / parameters | 12821 / 0 / 609 | 7272 / 0 / 473 |
| Goodness-of-fit on F ² | 1.062 | 1.063 |
| Final R indices [I > 2σ(I)] | R1 = 0.0276, wR2 = 0.0633 | R1 = 0.0262, wR2 = 0.0657 |
| R indices (all data) | R1 = 0.0361, wR2 = 0.0680 | R1 = 0.0280, wR2 = 0.0667 |
| Largest diff. peak and hole | 0.651 and -0.562 e Å ⁻³ | 0.842 and -0.659 e Å ⁻³ |